

## Uniplanar Orientations as a Tool To Assign Vibrational Modes of Polymer Chain

Alexandra R. Albulia, Paola Rizzo, and Gaetano Guerra\*

Dipartimento di Chimica, Università di Salerno,  
I-84084 Fisciano (SA), Italy

F. Javier Torres and Bartolomeo Civalleri

Dipartimento di Chimica IFM and NIS Center of Excellence,  
Università di Torino, Via P. Giuria 7, 10125 Torino, Italy

Claudio M. Zicovich-Wilson

Facultad de Ciencias, Universidad Autonoma Estado de  
Morelos, Av. Universidad 1001, 62210 Cuernavaca, Mexico

Received February 13, 2007

Revised Manuscript Received April 13, 2007

Energy (light frequency) and intensity of electronic and vibrational transitions are widely used in structural chemistry. On the other hand, polarization, i.e., the direction in the molecular framework of the transition moment vectors, is much less studied.<sup>1</sup> This is mainly due to the intrinsic difficulties in making polarization measurements, which need a molecular orientation control. For polymers, information relative to the direction in the molecular framework of the transition moment vectors is easily achieved by linear dichroism measurements on uniaxially stretched samples.<sup>2</sup> However, this method, which have been applied to most relevant polymers, is only able to discriminate between vibrational modes along the chain axis and perpendicular to the chain axis, while does not give any information relative to the direction of the transition moment vectors in the plane perpendicular to the chain axis.

Recently, for two crystalline phases ( $\gamma$  and  $\delta$ ) of syndiotactic polystyrene (s-PS) both containing  $s(2/1)2$  helices, films with three different kinds of uniplanar orientation have been achieved. In particular, as for the nanoporous  $\delta$  phase (Figure 1),<sup>3</sup> films with crystal planes (010),<sup>4</sup> (210),<sup>5</sup> or (002)<sup>6</sup> nearly parallel to the film plane, have been achieved by solvent treatment of biaxially stretched films,<sup>4a</sup> or by casting,<sup>4b,6a</sup> or by solvent induced crystallization.<sup>5,6b</sup> Also, we have anticipated by molecular simulations<sup>7</sup> and experimentally proved<sup>8</sup> that the orientation control of this nanoporous host phase allows one to control the kinetics of guest diffusion.

In this paper we show that (i) the occurrence of films with different uniplanar orientations of the crystalline phase allows an experimental evaluation of the orientation of transition moment vectors (TMV) of vibrational modes corresponding to most infrared peaks and that (ii) this information allows the difficult task of assignment of modes to vibrational peaks of complex polymer helices to be afforded.

A comparison between unpolarized FTIR spectra of  $\delta$ -form s-PS films both unoriented and with (002) orientation is reported in Figure 2, for two relevant spectral ranges. For the sake of simplicity, the present analysis have been confined to the range 1400–480  $\text{cm}^{-1}$ , which is the most conformationally sensitive spectral region.<sup>9</sup> For films presenting the (002) orientation (i.e., orientation of the polymer helices nearly perpendicular to the film plane) where the direction of the propagation of the light

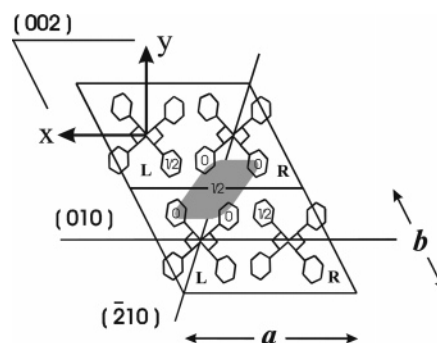


**Figure 1.** Along  $c$  view of two adjacent unit cells of  $\delta$  form s-PS: (002) crystal planes are parallel while (010) and (210) planes are perpendicular to the figure. Films with (010), (210), and (002) uniplanar orientations present these crystal planes nearly parallel to their surface. The  $x$  and  $y$  directions are parallel to the 2-fold axes perpendicular to the helical-chain axis, while the  $z$  direction is parallel to the chain axis.

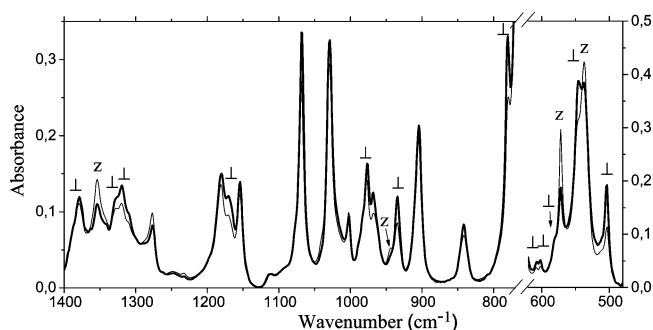


**Figure 2.** FTIR spectra in the wavenumber ranges 1400–770  $\text{cm}^{-1}$  and 630–480  $\text{cm}^{-1}$  of  $\delta$  form films: (thin line) unoriented and (thick line) with (002) uniplanar orientation. Peaks corresponding to vibrational modes perpendicular and parallel to the helical chain axis and have been labeled by  $\perp$  and  $z$ , respectively.

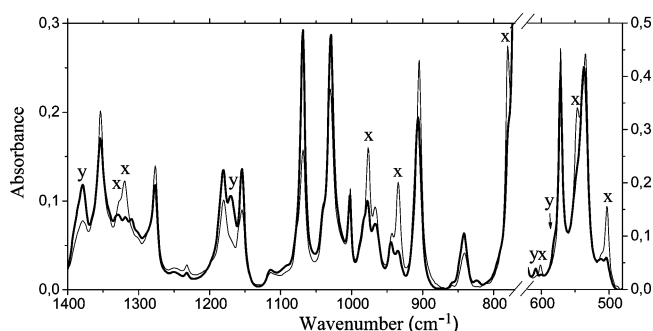


**Figure 3.** FTIR spectra of  $\delta$  form films with (thin line) (010) and (thick line) (210) uniplanar orientations. “Perpendicular” peaks corresponding to vibrational modes parallel and perpendicular to the  $a$  crystal axis are labeled as  $x$  and  $y$  (see Figure 1), respectively.

is nearly parallel to the chain axes, increased and reduced absorbances correspond to vibrational modes being perpendicular and parallel to the helical chain axis, respectively. Analogous information, of course, have been already achieved by linear dichroism measurements on uniaxially stretched films.<sup>9b</sup>

A comparison between unpolarized FTIR spectra of  $\delta$ -form s-PS films with (010) and (210) orientations is reported in Figure 3. On the basis of the knowledge of the crystalline structure of the  $\delta$ -form<sup>3a</sup> (see Figure 1), it is apparent that for films presenting the (010) orientation, because the direction of the propagation of the light is nearly perpendicular to this crystal plane (and hence also to the  $a$ -axis), “perpendicular” vibrational

\* Corresponding author. E-mail: gguerra@unisa.it.

**Table 1. FTIR Peak Positions ( $\nu$ ) and Experimental TMV Directions ( $\tau$ ) for  $\delta$ -Form s-PS Films Compared to the Corresponding Calculated Frequencies, TMV Directions, and Symmetries for an Infinite Chain of a s(2/1)2 Helix of s-PS (See Computational Details Section)**

$\nu_{\text{exp}}^a$	$\tau_{\text{exp}}^b$	$\nu_{\text{calc}}^a$	$\tau_{\text{calc}}^b$	symmetry <sup>c</sup>
1378	y	1383	y	B <sub>2u</sub>
1364	z	1366	z	B <sub>1u</sub>
1354	z	1358	z	B <sub>1u</sub>
1329	x	1329	x	B <sub>3u</sub>
1320	x	1320	x	B <sub>3u</sub>
1232	z	1231	z	B <sub>1u</sub>
1169	y	1167	y	B <sub>2u</sub>
1117	z	1098	z	B <sub>1u</sub>
1078	x	1078	x	B <sub>3u</sub>
977	x	969	x	B <sub>3u</sub>
944	z	934	z	B <sub>1u</sub>
934	x	921	x	B <sub>3u</sub>
858	z	853	z	B <sub>1u</sub>
780	x	769	x	B <sub>3u</sub>
766	z	765	z	B <sub>1u</sub>
750	x	743	x	B <sub>3u</sub>
601	x	594	x	B <sub>3u</sub>
581	y	577	y	B <sub>2u</sub>
572	z	566	z	B <sub>1u</sub>
548	x	540	x	B <sub>3u</sub>
534	z	530	z	B <sub>1u</sub>
503	x	498	x	B <sub>3u</sub>

<sup>a</sup> Values in  $\text{cm}^{-1}$ . <sup>b</sup> See Figure 1 for the definition of x, y and z TMV directions. <sup>c</sup> Rod group:  $P2_122$ .

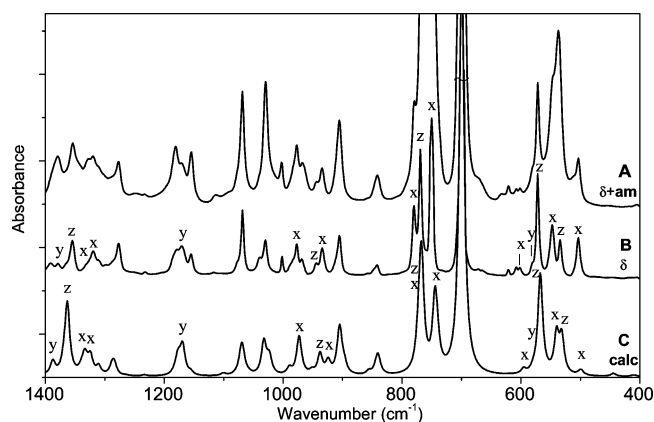
modes polarized along the  $x$  and  $y$  directions maximize and minimize their absorbances, respectively. On the other hand, for films presenting the  $(\bar{2}10)$  orientation, because the direction of the propagation of the light forms an angle of nearly  $17.5^\circ$  with the  $a$ -axis and hence with the  $x$  molecular direction (see Figure 1), “perpendicular” vibrational modes polarized along the  $x$  and  $y$  directions present reduced and increased absorbances, respectively.

Table 1 lists, for  $\delta$ -form s-PS films and only for the range  $1400\text{--}480\text{ cm}^{-1}$ , the infrared peaks whose TMV directions have been unambiguously established by the procedure discussed above (see Figures 2 and 3).

A common strategy to assign vibrational modes is to compare experiments with calculations. However, also for sophisticated ab initio calculations, that task can be difficult because of the presence of many vibrational modes within few wavenumbers and deviations relative to experimental peak positions larger than  $10\text{ cm}^{-1}$ . In this respect, the experimental evaluation of the directions of TMV for most FTIR peaks offers a powerful tool to facilitate vibrations assignment. In fact, although generally not used, the directions of TMV of vibrational modes can also be easily calculated.

Computed results at the B3LYP/6-31G(d,p) level of theory for an infinite chain model of a s(2/1)2 helix of s-PS are also reported in Table 1. The comparison between experimental and calculated TMV directions is then particularly relevant for complex polymer helices, which present a large number of vibrational peaks often superimposed in the observed and calculated spectra (e.g., for the s(2/1)2 helix of s-PS there are 141 IR-active vibrational modes).

FTIR spectra of an unoriented  $\delta$  form film of s-PS, before and after spectral subtraction of the amorphous phase contribution, are compared in Figure 4 along with the ab initio simulated spectrum (see Computational Details). The directions of the TMV, experimental and calculated are indicated close to curves B and C, respectively. The agreement between experimental and calculated spectra is satisfactory and it is, of course,



**Figure 4.** FTIR spectra: (A) of an unoriented  $\delta$  form film of s-PS; (B) spectrum A, after subtraction of the spectrum of the amorphous phase; (C) ab initio simulated spectrum of a s(2/1)2 helix of s-PS.

particularly good when the spectrum of the only crystalline phase (which contains only s(2/1)2 helices) is considered. Therefore, the presently available additional information, relative to the directions of the TMV, allows an unambiguous pairing between experimental and calculated infrared peaks, as shown in Table 1.

In perspective, the fruitful combination of experimental and calculation methods of the present study can be extended to other semicrystalline polymers with known crystalline structures. In particular, the experimental evaluation of TMV directions is possible for polymers, like, e.g., isotactic polypropylene or polyethyleneterephthalate, which can be shaped as films with at least one kind of uniplanar orientation with chain axis parallel to the film plane.

**Experimental Section.** Syndiotactic polystyrene was supplied by Dow Chemical under the trademark Questa 101.  $^{13}\text{C}$  nuclear magnetic resonance characterization showed that the content of syndiotactic polystyrene triads was over 98%. The weight-average molar mass obtained by gel permeation chromatography (GPC) in trichlorobenzene at  $135^\circ\text{C}$  was found to be  $M_w = 3.2 \times 10^5$  with the polydispersity index,  $M_w/M_n = 3.9$ .

All films considered in this paper present the nanoporous crystalline  $\delta$  phase and a thickness in the range  $20\text{--}40\text{ }\mu\text{m}$ . The films with uniplanar (010) and (002) orientations have been obtained by casting from 0.5 wt % solutions, at room temperature from chloroform<sup>4b</sup> and at  $50^\circ\text{C}$  from trichloroethylene,<sup>6a</sup> respectively. The film with uniplanar  $(\bar{2}10)$  orientation has been obtained by 1,4-dimethylnaphthalene diffusion at room temperature into an unoriented amorphous film.<sup>5</sup> The unoriented semicrystalline film has been obtained by THF diffusion in  $\gamma$  form films, in turn obtained by acetone treatment of an amorphous film.<sup>9d</sup>

Infrared spectra were obtained at a resolution of  $2.0\text{ cm}^{-1}$  with a Vector 22 Bruker spectrometer and/or with a Perkin-Elmer System 2000 spectrometer. Both instruments were equipped with a deuterated triglycine sulfate (DTGS) detector and a Ge/KBr beam splitter. The frequency scale was internally calibrated to  $0.01\text{ cm}^{-1}$  using a He–Ne reference laser. 32 scans were signal averaged to reduce the noise.

The degree of crystallinity of the used  $\delta$  form sPS films is in the range  $36\text{--}40\%$ , as evaluated according to the IR procedure described in ref 9d.

**Computational Details.** For the ab initio calculations on the  $\delta$ -form of s-PS, the adopted model consisted in an infinite one-dimensional s(2/1)2 helix that was constructed by the application of the symmetry operators of the  $P2_122$  rod group to its

irreducible part and the repetition of the resulting unit in the chain axis direction. Even if calculations could be performed on the crystalline structure, the adopted level of theory does not include dispersive effects needed for a correct description of the crystal packing. Therefore, for consistency, we decided to concentrate on the isolated infinite chain model that includes all of the most relevant vibrational modes.

The quantum mechanical calculations were carried out with the CRYSTAL06 code<sup>10</sup> by adopting the B3LYP functional together with a Gaussian Type all-electron 6-31G(d,p) basis set as level of theory. As a preliminary step, the atomic positions and the lattice constant were fully relaxed, and then, on the equilibrium geometry, the harmonic vibrational frequencies at the  $\Gamma$  point were subsequently computed by diagonalizing the mass-weighted Hessian matrix. On the basis of the  $P2_122$  rod group, whose factor group is isomorphous to  $D_{2h}$  point group, the computed frequencies were classified by symmetry and, according to the selection rules, the activity (or inactivity) of the modes in the IR spectrum was determined. Such a symmetry analysis is automatically performed by the CRYSTAL06 code.

The IR intensity  $A_i$  of any  $i$ th mode was calculated in the basis of the following definition:

$$A_i \propto d_i \left| \frac{\partial \mu}{\partial Q_i} \right|^2$$

It is proportional to the degeneracy  $d_i$  of the  $i$ th mode that multiplies the square of the first derivative of the cell dipole moment with respect to the normal mode coordinate  $Q_i$  (i.e., the Born charge tensor). The latter was computed numerically by using localized Wannier functions in the unit cell.<sup>11</sup> TMV directions were derived from the Cartesian Born charge tensor by computing the angle formed with the  $x$ ,  $y$ , and  $z$  axes, respectively.

In order to compare the computed and the experimental spectra, the resulting computed frequencies were scaled by a factor of 0.972 to best fit the experimental values in the selected region (i.e., 1400–480  $\text{cm}^{-1}$ ), then a graphical representation of the IR computed spectrum was obtained by using the calculated IR intensities and a Lorentzian profile (FWMH: 10  $\text{cm}^{-1}$ ).

**Acknowledgment.** Dr. Pellegrino Musto of CNR of Naples, Dr. Giuseppe Milano of University of Salerno, MIUR (Italy) (PRIN 2004) and “Regione Campania” (Legge 5 and CdCR) are gratefully acknowledged. CZW gratefully acknowledge financial support by CONACYT(Mexico) (Project SEP05-46983).

## References and Notes

- (1) (a) Piaggio, P.; Dellepiane, G.; Tubino, R.; Piseri, L.; Zannoni, G.; Zerbi, G.; Lugli, G. *J. Mol. Struct.* **1984**, *115*, 193–196. (b) Agosti, E.; Zerbi, G.; Ward, I. M. *Polymer* **1992**, *33*, 4219–29. (c) Michl, J.; Thulstrup, E. W. *Spectroscopy with polarized light*; VCH: New York, 1986. (d) Spanget-Larsen, J.; Thulstrup, E. W. *J. Mol. Struct.* **2003**, *661–662*, 603–610. (e) Albulia, A. R.; Di Masi, S.; Rizzo, P.; Milano, G.; Musto, P.; Guerra, G. *Macromolecules* **2003**, *36*, 8695–8703. (f) Albulia, A. R.; Milano, G.; Venditto, V.; Guerra, G. *J. Am. Chem. Soc.* **2005**, *127*, 13114–13115.
- (2) (a) Zbinden, R. *Infrared spectroscopy of high polymers*; Academic: New York, 1964. (b) Ward, I. M. *Structure and Properties of Oriented Polymers*, 2nd ed.; 1997.
- (3) (a) De Rosa, C.; Guerra, G.; Petraccone, V.; Pirozzi, B. *Macromolecules* **1997**, *30*, 4147–4152. (b) Milano, G.; Venditto, V.; Guerra, G.; Cavallo, L.; Ciambelli, P.; Sannino, D. *Chem. Mater.* **2001**, *13*, 1506–1511.
- (4) (a) Rizzo, P.; Albulia, A. R.; Milano, G.; Venditto, V.; Guerra, G.; Mensitieri, G.; Di Maio, L. *Macromol. Symp.* **2002**, *185*, 65–75. (b) Rizzo, P.; Lamberti, M.; Albulia, A.; Ruiz de Ballesteros, O.; Guerra, G. *Macromolecules* **2002**, *35*, 5854–5860.
- (5) Rizzo, P.; Spatola, A.; De Girolamo Del Mauro, A.; Guerra, G. *Macromolecules* **2005**, *38*, 10089–10094.
- (6) (a) Rizzo, P.; Costabile, A.; Guerra, G. *Macromolecules* **2004**, *37*, 3071–3076. (b) Rizzo, P.; Della Guardia, S.; Guerra, G. *Macromolecules* **2004**, *37*, 8043–8049.
- (7) (a) Milano, G.; Guerra, G.; Müller-Plathe, F. *Chem. Mater.* **2002**, *14*, 2977–2982. (b) Tamai, Y.; Fukuda, M. *Chem. Phys. Lett.* **2003**, *371*, 620–625.
- (8) (a) Venditto, V.; De Girolamo Del Mauro, A.; Mensitieri, G.; Milano, G.; Musto, P.; Rizzo, P.; Guerra, G. *Chem. Mater.* **2006**, *18*, 2205–2210. (b) Annunziata, L.; Albulia, A. R.; Venditto, V.; Mensitieri, G.; Guerra, G. *Macromolecules* **2006**, *39*, 9166–9170.
- (9) (a) Guerra, G.; Musto, P.; Karasz, F. E.; MacKnight, W. J. *Makromol. Chem.* **1990**, *191*, 2111–2119. (b) Reynolds, N. M.; Hsu, S. L. *Macromolecules* **1990**, *23*, 3463–3472. (c) Gowd, E. B.; Nair, S. S.; Ramesh, C.; Tashiro, K. *Macromolecules* **2003**, *36*, 7388–7397. (d) Albulia, A. R.; Musto, P.; Guerra, G. *Polymer* **2006**, *47*, 234–242.
- (10) Dovesi, R.; Saunders, V. R.; Roetti, C.; Orlando, R.; Zicovich-Wilson, C. M.; Pascale, F.; Civalieri, B.; Doll, K.; Harrison, N. M.; Bush, I. J.; D’Arco, P.; Llunell, M. *CRYSTAL06 User’s Manual*; Università di Torino: Torino, Italy, 2006.
- (11) (a) Zicovich-Wilson, C. M.; Dovesi, R.; Saunders, V. R. *J. Chem. Phys.* **2001**, *115*, 9708–9719. (b) Zicovich-Wilson, C. M.; Bert, A.; Dovesi, R.; Saunders, V. R. *J. Chem. Phys.* **2002**, *116*, 1120–1127.

MA070380+